

Effects of Resveratrol on the Structure and Catalytic Function of Bovine Liver catalase (BLC): Spectroscopic and Theoretical Studies

Samaneh Rashtbari¹, Gholamreza Dehghan^{1*}, Reza Yekta¹, Abolghasem Jouyban², Mehrdad Iranshahi³

¹ Department of Biology, Faculty of Natural Sciences, University of Tabriz, Tabriz, Iran.

² Pharmaceutical Analysis Research Center and Faculty of Pharmacy, Tabriz University of Medical Sciences, Tabriz, Iran.

³ Department of Pharmacognosy, Faculty of Pharmacy, Mashhad University of Medical Sciences, Mashhad, Iran.

Article info

Article History:

Received: 7 May 2017
Revised: 25 June 2017
Accepted: 5 July 2017
ePublished: 25 September 2017

Keywords:

- Bovine liver catalase
- Molecular docking
- Spectroscopy
- Trans resveratrol
- Uncompetitive inhibition

Abstract

Purpose: The study on the interaction between various compounds and macromolecules such as enzymes has been very important for monitoring the alteration of structural and functional properties of them. Resveratrol (3, 5, 4-trihydroxy-stilbene; RES) is a biologically active phytoalexin found in grapes and other food products. This article shows an interaction of native bovine liver catalase (BLC) with natural antioxidant product, trans resveratrol (tRES) using multispectroscopic methods.

Methods: The interaction between BLC and tRES is performed using UV-vis absorption, fluorescence and circular dichroism (CD) spectroscopy and molecular docking study.

Results: *In vitro* kinetic studies indicated that tRES can decrease BLC activity through uncompetitive inhibition. The results of spectroscopic methods represented that the binding of tRES with BLC can change the micro-region around aromatic amino acids (tryptophan (Trp) and tyrosine (Tyr)) and quench intrinsic fluorescence of BLC by a static mechanism. According to fluorescence quenching data analysis, it was revealed that tRES has one binding site on BLC. The thermodynamic parameters were obtained, which demonstrated that tRES can bind to BLC by van der Waals forces and hydrogen bonds. Molecular docking results indicated that tRES binds to BLC away from heme group and near to the Tyr 324 and Phe 265. These results are in agreement with the experimental results.

Conclusion: The inhibitory effect of tRES on BLC demonstrated that excessive consumption of the antioxidants could be resulted in hazardous effects.

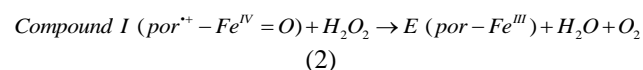
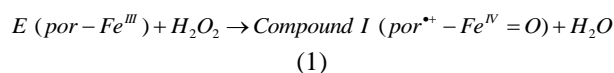
Introduction

Catalase (H₂O₂:H₂O₂ oxidoreductase, EC 1.11.1.6), one of the main components of the antioxidative defense system, is an active and ubiquitous enzyme that exists in almost all living organisms. It protects human and animal tissues against toxic effects of hydrogen peroxide (H₂O₂) that acts as a free radical.^{1,2} Catalase deficiency leads to many disorders such as aging, mutagenesis, acatalasemia, urinary tract diseases, diabetes, Alzheimer's disease, vitiligo and tumors.³

Bovine liver catalase (BLC) is a homotetramer enzyme with four subunits. Each subunit has over 506 amino acids, one NADPH molecule (as a cofactor) and protoporphyrin IX (the active-site heme group) containing a Fe³⁺.^{4,5} Heme group is vital for enzymatic reactions. Also, each subunit has four domains: β-barrel, N-terminal threading arm, wrapping loop and C-terminal helices. The β-barrel core structures are conserved in all catalases and heme group with a histidine (His), a tyrosine (Tyr) and an asparagine (Asn) is buried in the core structure.^{4,6} Catalase binds NADPH at a cleft between the β-barrel and helical domain on the surface of the molecule. NADPH is not necessary for the activity

of catalase and prevents inactivating of enzyme at low concentration of H₂O₂.⁴

There are three channels in catalase structure, which one of them reaches the active site. Through this channel substrate (H₂O₂) can enter and products can exist. Catalase catalyzes dismutation of H₂O₂ in two-step: in the first step, equation (1), one H₂O₂ molecule is reduced by ferricatalase (resting form of the enzyme), producing oxy-ferryl intermediate with a porphyrin π-radical cation, compound I, and H₂O molecule. In the second step, equation (2), compound I is reduced by another H₂O₂ molecule, result in formation resting form of enzyme and generation of O₂ and second H₂O molecule.⁷⁻⁹



*Corresponding author: Gholamreza Dehghan, Tel: +98 41 33392739, Email: gdehghan@tabrizu.ac.ir

©2017 The Authors. This is an Open Access article distributed under the terms of the Creative Commons Attribution (CC BY), which permits unrestricted use, distribution, and reproduction in any medium, as long as the original authors and source are cited. No permission is required from the authors or the publishers.

Human erythrocyte catalase (HEC) is very similar (similarity of 91%) to BLC, with the only difference in 43 amino-acid residues at the C-terminus domain.

Resveratrol (3,5,4-trihydroxy-stilbene; RES), as a natural polyphenolic product, belong to a group of phytochemicals called "stilbenoid".¹⁰ Stilbenoids are a subclass of phytoalexins and are produced by plants in response to injury, insect infestation, pathogens attack and ultraviolet exposure. RES found as two configurations: *trans*-(E) and *cis*-(Z)¹¹ (Figure 1). The *trans* form is more active and stable than *cis* form. It widely exists in most of the foods, particularly in grape skin, cranberries, blueberries and red wine.¹² *In vivo* studies showed that RES has beneficial effects such as anticancer effects that inhibit growth and proliferation of cancer cells by inhibiting angiogenesis and inducing apoptosis.¹³ It has other beneficial effects on the human body, including antioxidant activity (in the treatment of diabetes and obesity),¹⁴ cytoprotective,¹⁵ anti-inflammatory¹⁶ and anti-aging effects. Also, recently RES has shown neurodegenerative effects in experimental animals against neurological disorders such as Huntington, Parkinson and Alzheimer diseases.¹⁷ Shen et al. reported that RES can inhibit α -amylase and α -glucosidase in an uncompetitive manner.¹⁸

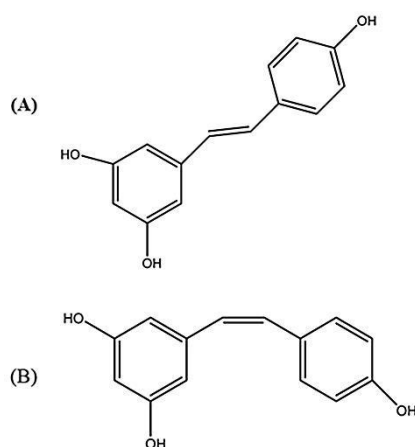


Figure 1. Resveratrol (3, 5, 4-trihydroxy- stilbene); (A) *trans*-(E) resveratrol, (B) *cis*-(Z) resveratrol.

The aim of this work was to investigate the possible effects of tRES on the structure and catalytic function of catalase by different methods. Since catalase exists at a high level in liver and this organ is one of the most important organs in the body, in which are metabolized and detoxified chemical and natural compounds, therefore study the side effects of varies drugs and compounds on catalase can be important. In this work we focus on the effects of tRES, as a natural occurring stilbene in fruits and beverages, on the structure and the activity of BLC.

Materials and Methods

Bovine liver catalase (BLC, MW; 250 KD) and dimethylsulfoxide (DMSO) were obtained from Sigma-Aldarich (St. Louis, MO, USA). Hydrogen peroxide

(H₂O₂) 30%, disodium hydrogen phosphate (MW; 177.99 g.mol⁻¹) and sodium dihydrogen phosphate (MW; 156.02 g.mol⁻¹) used in the buffer preparation were obtained from Merck Co. (Darmstadt, Germany). *Trans* resveratrol was purchased from Changsha Herbal Ingredient Co. (Changsha, China). The tRES stock solution (8.7 mM) was prepared by dissolving in DMSO. The concentration of the H₂O₂ stock solution was calculated by using its absorbance at 240 nm and the extinction coefficient of 40 M⁻¹ cm⁻¹.¹⁹ All chemicals used for the assays were chemically pure.

Kinetics studies of the native BLC

BLC activity was measured spectrophotometrically (T60, PG Instruments LTD., Leicestershire, UK) using the decrease in H₂O₂ maximum absorbance at 240 nm (A₂₄₀) due to its degradation by BLC.²⁰ In order to measure the BLC activity, the reaction mixture containing 50 mM sodium phosphate buffer (pH 7) and an appropriate amount of H₂O₂ (10-90 mM) were added to three ml cuvette. The enzymatic reactions were started by adding 10 μ l of BLC suspension (3 nM) to the mixtures. Changes at A₂₄₀ were recorded every two second for one minute and these alterations were considered as BLC activity.

In order to determine the possible effects of tRES on BLC activity, 3 nM of BLC in sodium phosphate buffer (pH 7) was incubated with various concentrations of tRES (2.9, 5.8, 8.7, 11.6 and 14.5 μ M). Subsequently, fixed concentration of H₂O₂ (60 mM) was added to the incubated solutions and changes in A₂₄₀ were recorded.

Spectroscopic studies

The UV-vis absorption spectra of BLC were recorded by UV-visible spectrophotometer (T60, PG Instruments LTD., Leicestershire, UK) in the range of 200-500 nm. In order to investigate the effects of tRES on BLC structure, its absorption spectra were recorded in the presence of different concentrations of tRES.

In order to monitor the structural changes of BLC in the presence of different concentrations of tRES (0.65, 1.31, 1.97, 2.62, 3.28, 3.94 and 4.59 μ M), all fluorescence spectra were recorded on (Jasco, FP-750 spectrofluorometer, Kyoto, Japan) at two temperatures (25 °C and 37 °C). The excitation wavelength (λ_{ex}) was fixed at 295 nm and emission wavelength (λ_{em}) was recorded from 300-500 nm.

According to the inner filter effect (IFE) definition, if a sample shows significant absorption at excitation and emission wavelengths, these effects should be corrected. Since IFE can be neglected for weak absorbance (i.e. weak concentrations), a common procedure is to dilute the solution until maximal absorbance is inferior than 0.1. Also, when the absorbance of the solution is lower than 0.3 the equation (3) can be used to correct the IFE.²¹

$$F_{cor} = F_{obs} \times 10^{\frac{(A_{ex} + A_{em})}{2}} \quad (3)$$

where F_{cor} and F_{obs} are the correct and observed fluorescence intensity, respectively. A_{ex} and A_{em} indicate the sample (tRES) absorbance at the excitation and emission wavelength, respectively.

In the present work, we diluted the stock solution of tRES until maximal absorbance at excitation wavelength (295 nm) and maximum emission wavelength of BLC (332 nm) was lower than 0.3.

Synchronous fluorescence spectra of BLC in the presence or absence of different concentrations of tRES was recorded using $\Delta\lambda=15$ nm with $\lambda_{em}=240-400$ for tyrosine (Tyr) and $\Delta\lambda=60$ nm with $\lambda_{em}=300-500$ for tryptophan (Trp). The scan speed was set at 1000 nm.min⁻¹.

Circular dichroism (CD) spectra of BLC in the presence and absence of tRES were measured by a circular dichroism spectropolarimeter (Jasco (J-810), Tokyo, Japan) at 25 °C in 50 mM sodium phosphate buffer, pH 7. In order to estimate the changes in the percentage of secondary structures of BLC under the effects of various concentrations of tRES, the CDNN software was used.

Molecular docking study

In order to predict the mode of interaction between tRES and BLC, molecular docking calculations were carried out using Auto Dock 4.2 software.²² The crystal structure of BLC was obtained from the Protein Data Bank (PDB Id: 1TGU). The molecular structure of tRES was generated using Hyperchem 8.0.6 program and was optimized for minimal energy by Gaussian 98 program. The Lamarckian genetic algorithm was applied to searching the optimum binding site of tRES to the BLC.²³ In order to recognize the binding sites in BLC, blind docking was carried out with setting of grid box size 126 Å³ (126 Å × 126 Å × 126 Å) grid points and 0.375 Å spacing. The VMD and Auto Dock Tools 1.5.4 packages were used for theoretical analysis of modes of interaction between BLC and tRES.²⁴

Results and Discussion

Kinetics studies

Analysis of BLC activity

BLC breakdowns H₂O₂ to H₂O and O₂. Decomposition of H₂O₂ by BLC leads to decrease in H₂O₂ UV absorption and this reduction was considered as BLC activity. For this purpose, a fixed concentration of BLC (3 nM) in the presence of additional concentration of H₂O₂ was used. The results showed that with increasing H₂O₂ concentration, enzyme activity increases (at low H₂O₂ concentration) and a linear relationship between enzyme activity and substrate concentration was observed (from 10 to 70 mM) but at higher concentrations of H₂O₂ (more than 70 mM), a marked reduction in enzyme activity was observed. This reduction is due to suicide inactivation of BLC by H₂O₂.²⁰ Michaelis-Menten and Lineweaver-Burk graphs were plotted and kinetic parameters were calculated according to Lineweaver-Burk graph and equation (4):

$$\frac{1}{V} = \frac{k_m}{V_{max}} \cdot \frac{1}{[S]} + \frac{1}{V_{max}} \quad (4)$$

The V_{max} and K_m values were determined to be 2.28 mM.S⁻¹ and 39 mM, respectively. Using the equation (5) the value of the catalytic constant (K_{cat}) was obtained as 7.6×10^5 s⁻¹.

$$V_{max} = k_{cat} \cdot [E_t] \quad (5)$$

Effect of tRES on BLC activity

In order to monitor the effect of tRES on BLC activity, enzyme activity was determined in the presence of various concentrations of tRES (2.9, 5.8, 8.7, 11.6 and 14.5 μM) and fixed concentration of H₂O₂ (70 μM). We observed that with increasing concentration of tRES, BLC activity significantly decreased (Figure 2A). The IC₅₀ value (the concentration of an inhibitor that inhibits 50% of the enzyme activity) was calculated as 8.1 μM (Figure 2A).

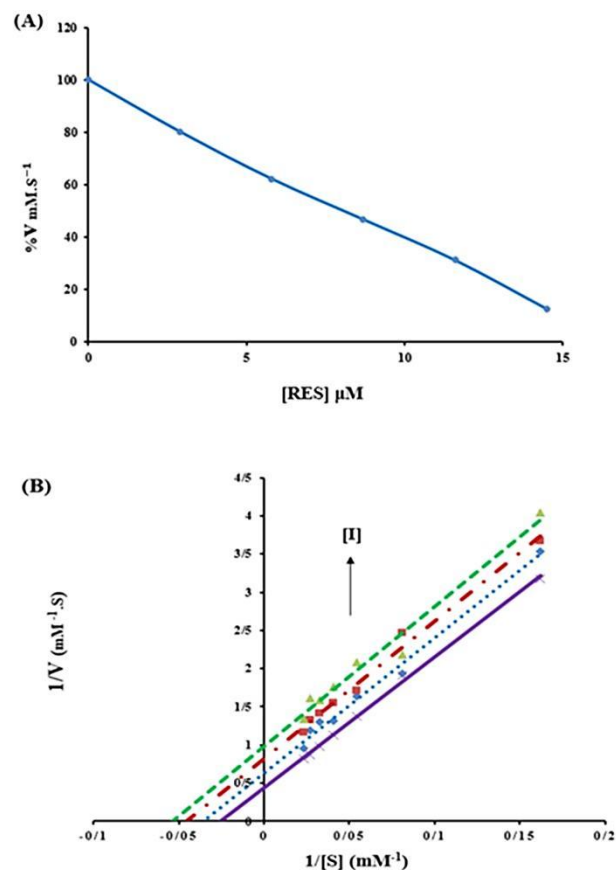


Figure 2. (A) The effect of various concentrations of tRES (0, 2.9, 5.8, 8.7, 11.6 and 14.5 μM) on the activity of BLC in 50 mM phosphate buffer, pH 7 at 25 °C. (B) Lineweaver-Burk plot of BLC (3 nM) with and without various concentrations of tRES: 0 (×), 4.05 (•), 8.1 (■) and 16.2 (▲) μM in 50 mM phosphate buffer, pH 7, 25 °C.

There are three types of reversible enzyme inhibition mechanism: competitive, in which inhibitor binds to the free enzyme and competes with the substrate, non-competitive in which inhibitor interacts with both the

free enzyme and enzyme-substrate (ES) complex and uncompetitive (also named anticompetitive inhibition) in which inhibitor only binds to the ES complex.²⁵ In order to estimate the enzyme inhibition mechanism, enzyme activity in the presence of different concentrations of tRES was measured and Lineweaver-Burk graphs were plotted. According to these plots and using equation (6), the kinetic parameters (K_m^{app} and V_m^{app}) were calculated (Table 1) and compared with kinetic parameters of untreated BLC (Table 1). Lineweaver-Burk equation for uncompetitive inhibition is:²⁶

$$\frac{1}{V_0} = \frac{k_m}{V_{max}} \cdot \frac{1}{[S]} + \frac{1}{V_{max}} \cdot \left(1 + \frac{[I]}{K_i}\right) \quad (6)$$

The results showed that with increasing concentration of tRES, K_m^{app} and V_m^{app} values decreased, which is characteristic of an uncompetitive inhibitor (Figure 2B).

Table 1. The V_m and K_m values of BLC with and without tRES.

Concentration of RES(μ M)	V_m (mM.s ⁻¹)	K_m (mM)
0	2.28	39
4	1.57	27.7
8	1.21	21.69
16	1.01	18.48

UV-vis absorption spectrophotometry

UV-vis spectrophotometry, as an impressive and simple technique, is used to monitoring the conformational changes of macromolecules (such as proteins) that occur upon interaction with various ligands.²⁷ Most of the proteins such as BLC show main absorption bands around 280 nm, which are caused by the existence of aromatic amino acids including tryptophan (Trp), phenylalanine (Phe) and tyrosine (Tyr).²⁸ Also, BLC has an important absorption peak around 405 nm (Soret-band) due to $\pi \rightarrow \pi^*$ transition of electrons in the porphyrin ring of heme group. In this study, UV-vis absorption spectra of BLC were recorded (1 μ M) in the presence of three concentrations of tRES (4.05, 8.1 and 16.2 μ M). Figure 3 shows that in the presence of additional concentration of tRES, absorption intensity around 405 nm (Soret-band) increases regularly (a little hyperchromic shift) compared with the native enzyme. Slight increase in the absorption peak of Soret-band indicates that no significant structural change of BLC occurs and tRES cannot directly bind to the deeply buried heme group. The Soret-band is sensitive to alterations of the microenvironment of heme group, so a small displacement of Soret-peak observed in the presence of tRES, indicating a little alteration in the microenvironment of tryptophan residue.^{29,30} Due to the overlapping of BLC and tRES bands around 280 nm, it was not feasible to estimate the alteration at 280 nm, therefore we used fluorescence spectroscopy.

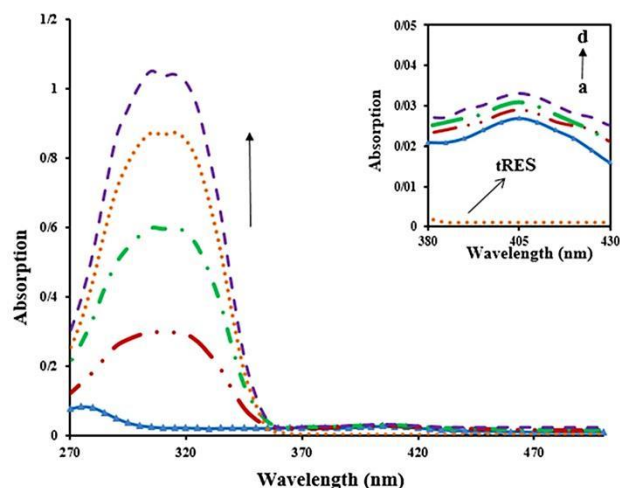


Figure 3. UV-vis absorption spectra of BLC (1 μ M) in the absence and presence of additional concentration of tRES and a magnified image of the Soret-bands: (a) 0, (b) 4.05, (c) 8.1 and (d) 16.2 μ M in 50 mM phosphate buffer, pH 7, 25 °C.

Fluorescence spectroscopy

This method is used to conformational changes studies of proteins. Three aromatic amino-acids (Trp, Tyr and Phe) exist in protein structure and contribute to their intrinsic fluorescence emission. The emission of tryptophan is highly dependent on polarity and local environment whereas the emission of tyrosine is insensitive to solvent polarity. The effect of Phe on protein's fluorescence is less than others.²⁸ In order to investigate the effect of tRES on fluorescence intensity of BLC (0.7 μ M), the additional concentration of tRES (0-5.0 μ M) was used and excitation wavelength was set at 295 nm. Also, the studied emission wavelength was 322 nm (maximum emission wavelength of BLC).

When the excitation wavelength is set at 295 nm, the effect of Tyr is overlooked. We observed that tRES leads to quenching of intrinsic fluorescence of BLC due to alteration in the surrounding environment of Trp. Also, the results suggest that tRES and BLC form a new complex (Figure 4A). Since tRES had significant absorption at excitation and maximum emission wavelength of BLC, the inner filter effects were corrected according to equation (3) (Figure 4B).

Quenching mechanisms (static and dynamic quenching) are determined using their different dependence on temperature. In static quenching, the bimolecular quenching constant decreases with increasing temperature. Dynamic fluorescence quenching is a diffusion process and therefore the value of quenching constants increase with increasing temperature.³¹ As shown in (Figure 4B), the quenching mechanism is static. In order to confirm the quenching mechanisms, Stern-Volmer equation (equation (7)) was used:³²

$$\frac{F_0}{F} = 1 + K_{sv}[Q] = 1 + K_q\tau_0[Q] \quad (7)$$

where F and F_0 are the fluorescence intensities of BLC with and without the quencher (tRES), respectively, $[Q]$

is the concentration of the quencher, K_q is the quenching rate constant of the biomolecule and K_{SV} is the Stern–Volmer quenching constant and τ_0 is the fluorescence lifetime without quencher, which is 10^{-8} s for BLC.³³ According to the plot of F_0/F vs. $[Q]$ (Figure 5), the values of K_{SV} and K_q at different temperatures were obtained and summarized in Table 2. The results showed

that, the K_{SV} values reduce with increasing temperature, and K_q values are greater than 2×10^{10} L mol⁻¹ s⁻¹ (maximum dynamic quenching constant). This result confirmed that the quenching is mostly static process and fluorescence quenching of BLC is due to formation of BLC-tRES complex in ground state.

Table 2. Binding and thermodynamic parameters of BLC and tRES complex at different temperatures (25 °C and 37 °C).

Temperature (°C)	n	$K_{SV} (\times 10^5 M^{-1})$	$K_q (\times 10^{14} M^{-1} s^{-1})$	$K (\times 10^3 M^{-1})$	$\Delta G \text{ kJmol}^{-1}$	$\Delta H \text{ kJmol}^{-1}$	$\Delta S \text{ JK}^{-1}\text{mol}^{-1}$
25	0.71	1.4	1.4	4.9	-21	-40	-63
37	0.69	1	1	2.6	-20		

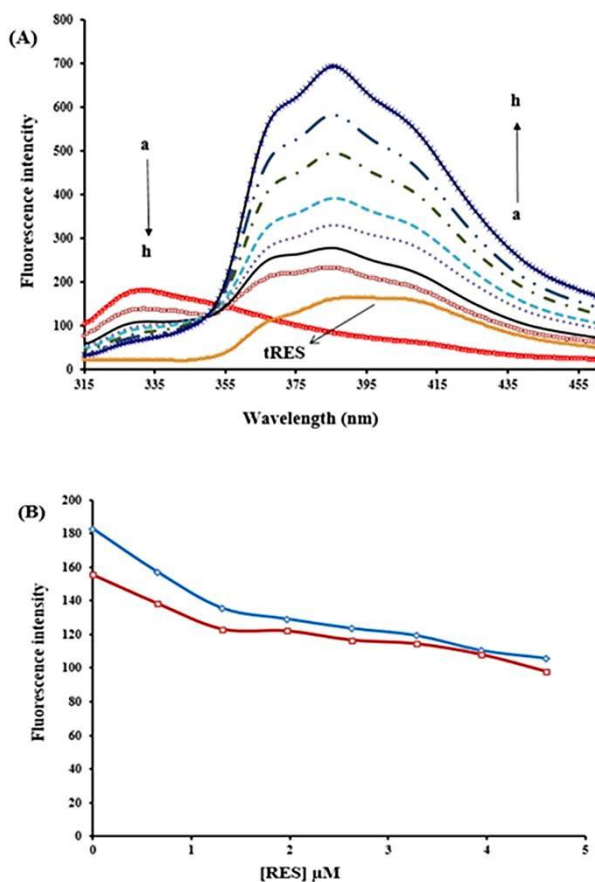


Figure 4. (A) Effect of various concentrations of tRES on fluorescence intensity of BLC. λ_{exc} =295, BLC concentration: (0.7 μ M); tRES concentrations:(a) 0, (b) 0.65, (c) 1.31, (d) 1.97, (e) 2.62, (f) 3.28, (g) 3.94, and (h) 4.59 μ M, (i) only RES, 0.65 μ M. (B) fluorescence quenching of BLC in the presence of various concentrations of tRES after correcting inner filter effect, pH 7.4, T=298 K (\blacklozenge), T=310 K (\blacksquare).

Synchronous fluorescence spectroscopy

Synchronous fluorescence is another simple and sensitive technique that provides important information about the microenvironment in the surrounding of the chromophore and conformational changes in proteins. In this technique, the spectra are recorded by scanning synchronously both emission and excitation wavelength, fixing wavelength interval ($\Delta\lambda$) between them.³⁴ The $\Delta\lambda$ can be selected 15 nm or 60 nm and synchronous fluorescence can give main information about microenvironment around the Tyr and

Trp, respectively. We observed that synchronous fluorescence spectra of BLC changed under the effect of tRES. As shown in (Figure 6A), with increasing concentration of tRES, the emission spectra of Tyr shifted to the smaller wavelength (blue shift) about 1 nm, which describes a little increase in the hydrophobicity of Tyr, leading to partially expose of heme group to solvent. The emission spectra of Trp shifted to longer wavelength (red shift) about four nm (Figure 6B), demonstrating a decrease of hydrophobicity in Trp micro-region and Trp residue transferred from nonpolar to polar environment.³⁵

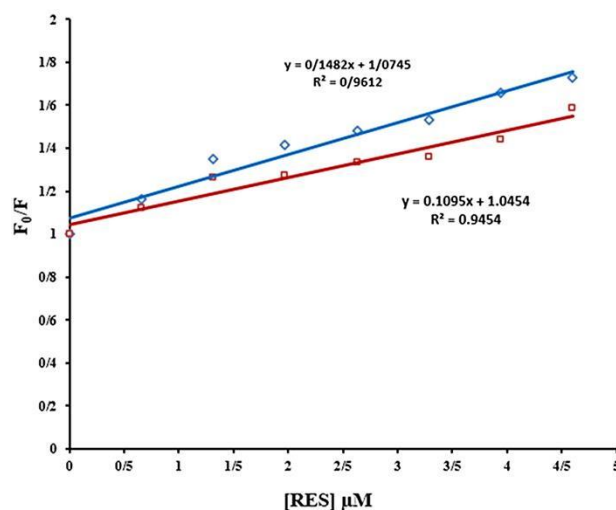


Figure 5. Stern-Volmer curve for quenching of BLC by various concentrations of tRES at 298 K (\blacklozenge) and 310 K (\blacksquare).

Circular dichroism spectroscopy study

In order to determine the secondary structure changes of BLC upon tRES binding, CD spectra in the far-UV region were recorded (Figure 7). The CD spectra of BLC show two main negative bands at 208 nm and 222 nm (due to $\pi \rightarrow \pi^*$ transition which occurs in the peptide chain). Those are characteristic of an alpha helical structure of the BLC. Also, BLC with β -pleated sheets shows a negative band at 218 nm, while random coils have very low ellipticity above 210 nm.³⁶ BLC consist of the secondary conformation of 27.4% α -helix, 21.2% β -pleated sheet, 17.6% β -turn and 33.8% random coil. The results showed that secondary structures of BLC change (a little) in the presence of tRES. The effects of tRES on

the percentage of secondary structural elements in BLC were summarized in Table 3. According to the data of Table 3, tRES had no significant effect on the secondary structure of BLC.

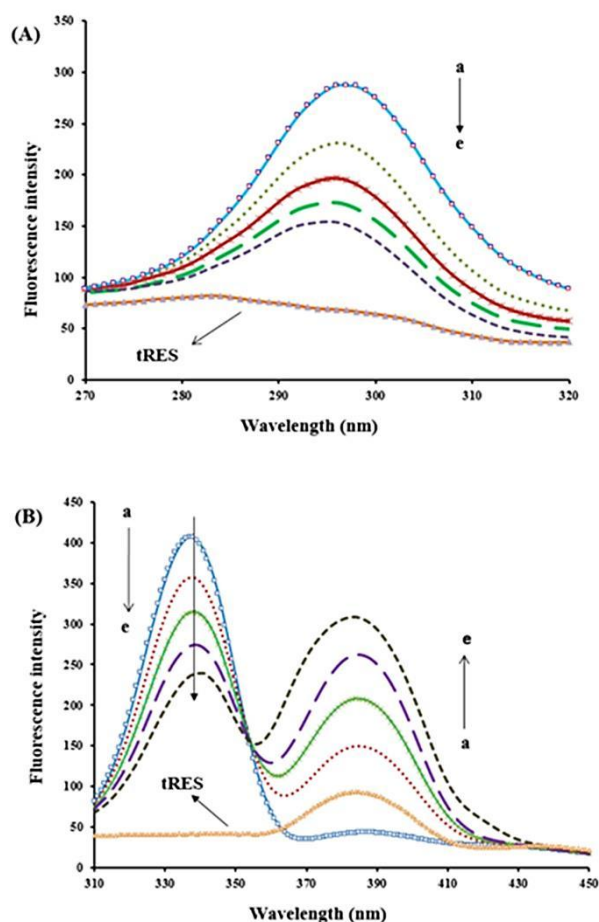


Figure 6. Synchronous fluorescence spectra of BLC in the presence of additional concentration of tRES (a) 0, (b) 0.65, (c) 1.31, (d) 1.97 and (e) 2.62 μM; (A) $\Delta\lambda=15$ and (B) $\Delta\lambda=60$ nm, (f) only RES 0.6 μM, pH 7.4, T=298 K.

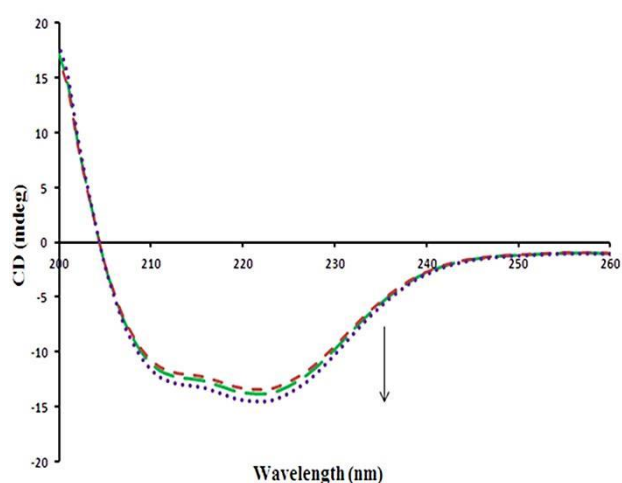


Figure 7. CD spectra of BLC in the absence and presence of tRES at 298 K (25 °C).

Table 3. The percentage of secondary structure elements of BLC in the presence and absence of tRES at 298 K (25 °C).

[tRES] μM	Secondary structure content in BLC (%)			
	α-helix	β-sheet	β-turns	random coil
0	27.4	21.2	17.6	33.8
10	27.6	21	17	33.3
20	28.3	20.4	18.8	33.6

Analysis of binding mode and thermodynamic

For the static quenching mechanism, the number of binding sites (n) and binding constant (K) can be calculated by the following equation (8):

$$\log \frac{F_0 - F}{F} = \log K + n \log [Q] \quad (8)$$

The " n " and K values were determined by using the intercept and slope values of the plot $\log \frac{F_0 - F}{F}$ vs. $\log [Q]$ (Figure 8) and were listed in Table 2. The results showed that " n " value is approximately close to one, describe that one tRES molecule can bind to one BLC molecule and exist one binding site on BLC for tRES. The K values reduced by an increase in the temperature indicate that the stability of BLC and tRES complex lost. Also, K is of the order of 10^3 , indicates that there is a significant interaction between tRES and BLC.³⁰

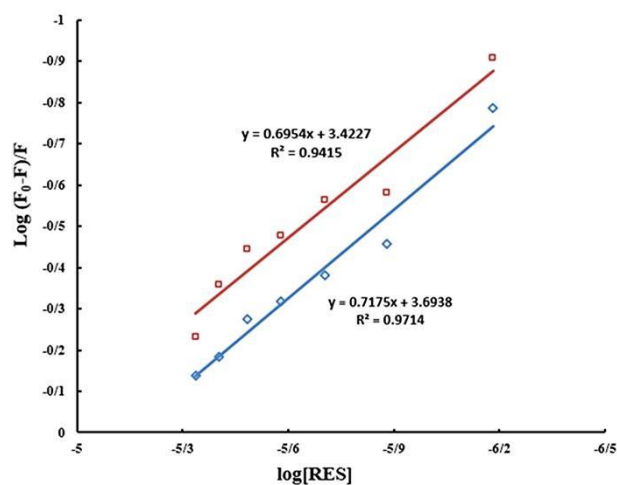


Figure 8. The linear plot of $\log \frac{F_0 - F}{F}$ vs. $\log [Q]$ for quenching of BLC in the presence of tRES at 298 K (♦) and 310 K (■).

The interaction forces between a ligand and a macromolecule mainly including: electrostatic interactions, hydrophobic interactions, van der Waals forces and hydrogen bonding. The type of acting forces is estimated on the base of the sign and amount of ΔH and ΔS (thermodynamic parameters): $\Delta H < 0$ and $\Delta S > 0$ suggest electrostatic forces are dominant; $\Delta H > 0$ and $\Delta S > 0$ indicate hydrophobic interactions are main; $\Delta H < 0$ and $\Delta S < 0$ imply van der Waals forces and hydrogen bonding are more important.¹⁹ Equations from (9) to (11), were applied to calculating the ΔH (enthalpy), ΔG (Gibbs

free energy) and ΔS (entropy) values, respectively, and the findings were summarized in Table 2.

$$\ln \frac{K_2}{K_1} = \frac{-\Delta H}{R} \left(\frac{1}{T_2} - \frac{1}{T_1} \right) \quad (9)$$

$$\Delta G = -RT \ln K \quad (10)$$

$$\Delta G = \Delta H - T\Delta S \quad (11)$$

The negative values for ΔG , ΔH and ΔS support the assumption that tRES binds to BLC spontaneously, the formation complex between them (BLC-tRES) is exergonic reaction and entropy reduces during the formation of complex, respectively.³⁰ Also, van der Waals forces and hydrogen bonds play main roles in this interaction.

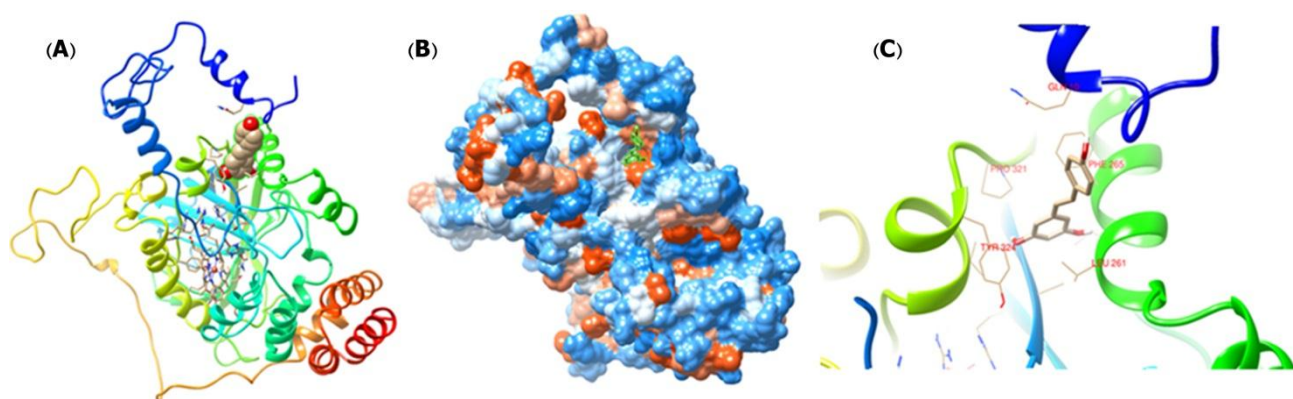


Figure 9. Molecular docking models for BLC-tRES complex (A) The structure of one subunit of BLC binding to tRES in carton form and (B) in hydrophobic surface model. (C) Detailed illustration of the binding between BLC and tRES.

Conclusion

The present work examined the effect of tRES on catalase structure and catalytic activity. *In vitro* studies indicated that, tRES can inhibit catalase activity by an uncompetitive mechanism and it spontaneously binds to BLC through one binding site. Spectroscopic results showed that tRES causes the conformational changes in BLC structure. Synchronous fluorescence, CD and UV-vis absorption spectroscopic studies suggested that the micro- region of Trp, Tyr and secondary structure of catalase change in the presence of tRES.

Fluorescence spectroscopy results suggest that with additional concentration of tRES, Trp residues are exposed to a less hydrophobic environment, due to unfolding of BLC structure upon interaction with tRES. Molecular docking calculation was applied in order to estimate the best mode of interaction between tRES and BLC, the binding energy of the interaction and the regions involved in the interaction, which the results show good agreements with the experimental binding studies data. Our results from thermodynamic studies indicated that tRES interacts with BLC through non-covalent and caused inhibition of the BLC activity.

Ethical Issues

Not applicable.

Molecular docking results

Molecular docking is one of the most important methods which predicts the best interaction between a ligand and macromolecule based on the lowest energy.³⁷ The molecular docking results illustrated that there are one binding site for tRES on BLC at a cavity among the β -barrel and helical domain which is away from heme group (Figure 9A and 9B). Also Figure 9C shows that in this interaction Phe 265 and Tyr 324 residues are involved. These results are in good agreement with results of UV absorption and fluorescence studies. Docking results indicate that hydrogen bonds and van der Waals forces contribute in interactions between BLC and tRES. The value of binding energy was obtained - 6.8 Kcal mol⁻¹ by docking calculation.

Conflict of Interest

The authors declare no conflict of interests.

References

- Chelikani P, Carpena X, Fita I, Loewen PC. An electrical potential in the access channel of catalases enhances catalysis. *J Biol Chem* 2003;278(33):31290-6. doi: 10.1074/jbc.M304076200
- Wang Y, Zhang H. Comprehensive studies on the nature of interaction between catalase and SiO₂ nanoparticle. *Mater Res Bull* 2014;60:51-6. doi: 10.1016/j.materresbull.2014.08.024
- Harifi-Mood AR, Ghobadi R, Divsalar A. The effect of deep eutectic solvents on catalytic function and structure of bovine liver catalase. *Int J Biol Macromol* 2017;95:115-20. doi: 10.1016/j.ijbiomac.2016.11.043
- Goyal MM, Basak A. Human catalase: looking for complete identity. *Protein Cell* 2010;1(10):888-97. doi: 10.1007/s13238-010-0113-z
- Chakravarti R, Gupta K, Majors A, Ruple L, Aronica M, Stuehr DJ. Novel insights in mammalian catalase heme maturation: EFFECT of NO and thioredoxin-1. *Free Radic Biol Med* 2015;82:105-13. doi: 10.1016/j.freeradbiomed.2015.01.030

6. Ko TP, Safo MK, Musayev FN, Di Salvo ML, Wang C, Wu SH, et al. Structure of human erythrocyte catalase. *Acta Crystallogr D Biol Crystallogr* 2000;56(Pt 2):241-5. doi: 10.1107/S0907444999015930
7. Switala J, Loewen PC. Diversity of properties among catalases. *Arch Biochem Biophys* 2002;401(2):145-54. doi: 10.1016/S0003-9861(02)00049-8
8. Mureşanu C, Copolovici L, Pogăcean F. A kinetic method for para-nitrophenol determination based on its inhibitory effect on the catalatic reaction of catalase. *Open Chem* 2005;3(4):592-604. doi: 10.2478/BF02475190
9. Krych J, Gebicka L. Catalase is inhibited by flavonoids. *Int J Biol Macromol* 2013;58:148-53. doi: 10.1016/j.ijbiomac.2013.03.070
10. Amri A, Chaumeil JC, Sfar S, Charrueau C. Administration of resveratrol: what formulation solutions to bioavailability limitations? *J Control Release* 2012;158(2):182-93. doi: 10.1016/j.jconrel.2011.09.083
11. Burns J, Yokota T, Ashihara H, Lean ME, Crozier A. Plant foods and herbal sources of resveratrol. *J Agric Food Chem* 2002;50(11):3337-40. doi: 10.1021/jf0112973
12. Huang X, Dai Y, Cai J, Zhong N, Xiao H, McClements DJ, et al. Resveratrol encapsulation in core-shell biopolymer nanoparticles: Impact on antioxidant and anticancer activities. *Food Hydrocoll* 2017;64:157-65. doi: 10.1016/j.foodhyd.2016.10.029
13. Cal C, Garban H, Jazirehi A, Yeh C, Mizutani Y, Bonavida B. Resveratrol and cancer: chemoprevention, apoptosis, and chemo-immunosensitizing activities. *Curr Med Chem Anticancer Agents* 2003;3(2):77-93. doi: 10.2174/1568011033353443
14. Tian X, Liu Y, Ren G, Yin L, Liang X, Geng T, et al. Resveratrol limits diabetes-associated cognitive decline in rats by preventing oxidative stress and inflammation and modulating hippocampal structural synaptic plasticity. *Brain Res* 2016;1650:1-9. doi: 10.1016/j.brainres.2016.08.032
15. Mallebrera B, Brandolini V, Font G, Ruiz MJ. Cytoprotective effect of resveratrol diastereomers in CHO-K1 cells exposed to beauvericin. *Food Chem Toxicol* 2015;80:319-27. doi: 10.1016/j.fct.2015.03.028
16. Csiszar A. Anti-inflammatory effects of resveratrol: possible role in prevention of age-related cardiovascular disease. *Ann N Y Acad Sci* 2011;1215:117-22. doi: 10.1111/j.1749-6632.2010.05848.x
17. Pasinetti GM, Wang J, Marambaud P, Ferruzzi M, Gregor P, Knable LA, et al. Neuroprotective and metabolic effects of resveratrol: therapeutic implications for Huntington's disease and other neurodegenerative disorders. *Exp Neurol* 2011;232(1):1-6. doi: 10.1016/j.expneurol.2011.08.014
18. Shen Y, Xu Z, Sheng Z. Ability of resveratrol to inhibit advanced glycation end product formation and carbohydrate-hydrolyzing enzyme activity, and to conjugate methylglyoxal. *Food Chem* 2017;216:153-60. doi: 10.1016/j.foodchem.2016.08.034
19. Moradi M, Divsalar A, Saboury AA, Ghalandari B, Harifi AR. Inhibitory effects of deferasirox on the structure and function of bovine liver catalase: a spectroscopic and theoretical study. *J Biomol Struct Dyn* 2015;33(10):2255-66. doi: 10.1080/07391102.2014.999353
20. Koohekan B, Divsalar A, Saiedifar M, Saboury AA, Ghalandari B, Gholamian A, et al. Protective effects of aspirin on the function of bovine liver catalase: A spectroscopy and molecular docking study. *J Mol Liq* 2016;218:8-15. doi: 10.1016/j.molliq.2016.02.022
21. Pacheco ME, Bruzzone L. Synchronous fluorescence spectrometry: Conformational investigation or inner filter effect? *J Lumin* 2013;137:138-42. doi: 10.1016/j.jlumin.2012.12.056
22. Morris GM, Huey R, Lindstrom W, Sanner MF, Belew RK, Goodsell DS, et al. AutoDock4 and AutoDockTools4: Automated docking with selective receptor flexibility. *J Comput Chem* 2009;30(16):2785-91. doi: 10.1002/jcc.21256
23. de Magalhães CS, Barbosa HJC, Dardenne LE. A genetic algorithm for the ligand-protein docking problem. *Genet Mol Biol* 2004;27(4):605-10. doi: 10.1590/S1415-47572004000400022
24. Humphrey W, Dalke A, Schulten K. VMD: visual molecular dynamics. *J Mol Graph* 1996;14(1):33-8. doi: 10.1016/0263-7855(96)00018-5
25. Cappiello M, Moschini R, Balestri F, Mura U, Del-Corso A. Basic models for differential inhibition of enzymes. *Biochem Biophys Res Commun* 2014;445(3):556-60. doi: 10.1016/j.bbrc.2014.02.030
26. Park YD, Kim SY, Lyoo YJ, Lee JY, Yang JM. A new type of uncompetitive inhibition of tyrosinase induced by Cl-binding. *Biochimie* 2005;87(11):931-7. doi: 10.1016/j.biochi.2005.06.006
27. Farajzadeh Dehkordi M, Dehghan G, Mahdavi M, Hosseinpour Feizi MA. Investigation on the Binding Mode of 3, 4-Dihydropyrano[c]Chromene Derivative with Double Strand DNA. *Adv Pharm Bull* 2015;5(4):477-81. doi: 10.15171/apb.2015.065
28. Lakowicz JR, Masters BR. Principles of fluorescence spectroscopy. *J Biomed Opt* 2008;13(2):029901.
29. Yang B, Hao F, Li J, Chen D, Liu R. Binding of chrysoidine to catalase: spectroscopy, isothermal titration calorimetry and molecular docking studies. *J Photochem Photobiol B* 2013;128:35-42. doi: 10.1016/j.jphotobiol.2013.08.006
30. Xu Q, Lu Y, Jing L, Cai L, Zhu X, Xie J, et al. Specific binding and inhibition of 6-benzylaminopurine to catalase: Multiple spectroscopic methods combined with molecular docking study. *Spectrochim Acta, Pt A: Mol Biomol*

- Spectrosc* 2014;123:327-35. doi: 10.1016/j.saa.2013.12.021
31. Yu Z, Liu H, Hu X, Song W, Liu R. Investigation on the toxic interaction of superparamagnetic iron oxide nanoparticles with catalase. *J Lumin* 2015;159:312-6. doi: 10.1016/j.jlumin.2014.10.049
32. Keizer J. Nonlinear fluorescence quenching and the origin of positive curvature in Stern-Volmer plots. *J Am Chem Soc* 1983;105(6):1494-8. doi: 10.1021/ja00344a013
33. Teng Y, Zhang H, Liu R. Molecular interaction between 4-aminoantipyrine and catalase reveals a potentially toxic mechanism of the drug. *Mol Biosyst* 2011;7(11):3157-63. doi: 10.1039/c1mb05271c
34. Teixeira AP, Duarte TM, Carrondo MJ, Alves PM. Synchronous fluorescence spectroscopy as a novel tool to enable PAT applications in bioprocesses. *Biotechnol Bioeng* 2011;108(8):1852-61. doi: 10.1002/bit.23131
35. Teng Y, Zou L, Huang M, Zong W. Molecular interaction of 2-mercaptobenzimidazole with catalase reveals a potentially toxic mechanism of the inhibitor. *J Photochem Photobiol B* 2014;141:241-6. doi: 10.1016/j.jphotobiol.2014.09.018
36. Greenfield NJ. Using circular dichroism spectra to estimate protein secondary structure. *Nat Protoc* 2006;1(6):2876-90. doi: 10.1038/nprot.2006.202
37. Thomsen R, Christensen MH. MolDock: a new technique for high-accuracy molecular docking. *J Med Chem* 2006;49(11):3315-21. doi: 10.1021/jm051197e